Journal of Applied Electrochemistry (2005) 35:157–162
DOI 10.1007/s10800-004-6301-x

Physical and electrochemical characteristics of nanostructured nickel hydroxide powder

Q.S. SONG[1]*, Y.Y. LI[2] and S.L.I. CHAN[3]
[1]*Department of Applied Chemistry, School of Chemical Engineering and Technology, Tianjin University, Tianjin 300072, P.R. China*
[2]*Department of Materials Science and Engineering, National Taiwan University, Taipei 106, Taiwan*
[3]*School of Materials Science and Engineering, University of New South Wales, Sydney, NSW 2052, Australia*
*(*author for correspondence, fax: +86-22-27403389, e-mail: weisu@public.tpt.tj.cn)*

Received 30 March 2004; accepted in revised form 01 October 2004

Key words: chemical precipitation reaction, electrochemical activity, nanostructured material, nickel hydroxide, pasted nickel electrode, structural characteristics

Abstract

Nanostructured nickel hydroxide powder has been synthesized by a chemical precipitation method with the aid of ultrasound radiation, and the physical properties of the synthesized material were characterized by scanning electron microscopy, specific surface area, X-ray diffraction and differential scanning calorimetry. It was found that nanostructured nickel hydroxide was crystalline β-Ni(OH)$_2$ with a nanocrystalline and nanoporous surface structure. The crystallite sizes of nanostructured β-Ni(OH)$_2$ along the *c*- and *a*-axis were 2.5 and 2.3 nm, respectively, as calculated from (001) and (100) X-ray diffraction peaks. In comparison with spherical β-Ni(OH)$_2$ which has now been widely used as the active material for pasted nickel electrodes, nanostructured β-Ni(OH)$_2$ possessed a smaller crystallite size, more structural defects, a larger lattice parameter of c_0, a higher specific surface area and lower thermal decomposition temperature. These physical characteristics were advantageous to the improvement of electrochemical activity of the nanostructured nickel hydroxide powder. Studies indicated that the filling property and flowability of nanostructured β-Ni(OH)$_2$, which were characterized by the measurements of tapping density and angle of repose, were inferior to those of spherical β-Ni(OH)$_2$. Pasted nickel electrodes with a porous nickel-foam substrate were prepared using a mixture of the nanostructured and spherical Ni(OH)$_2$ powders as the active material. Charge/discharge tests showed that the addition of an appropriate amount of nanostructured Ni(OH)$_2$ powder to spherical Ni(OH)$_2$ powder could enhance the specific discharge capacity and high-rate capability of the pasted nickel electrodes. This enhancement could be attributed to a lowered electrochemical reaction impedance for the nickel electrode with the addition of nanostructured Ni(OH)$_2$ relative to the electrode without nanostructured Ni(OH)$_2$.

1. Introduction

Nickel hydroxide and nickel oxide materials have received increasing attention in recent years on account of their applications in alkaline secondary batteries, fuel cells, electrochemical capacitors, electrolyzers, electrosynthetic cells and electrochromic devices [1–5]. Rechargeable alkaline nickel batteries (e.g. Ni/Cd, Ni/Fe, Ni/Zn, Ni/H$_2$ and Ni/MH) are usually positive limited, so that the capacity and cycle life of the cells are determined mainly by the properties of nickel electrodes. In order to improve the cell performance, pasted nickel electrodes made from a porous nickel-foam substrate and an active material called spherical nickel hydroxide powder have been developed [6, 7]. With their high energy density and low cost relative to those of conventional sintered nickel electrodes, the pasted nickel electrodes have now been widely used in commercially available Ni/MH and Ni/Zn batteries.

As the discharged-state active material of the nickel electrodes, the physical and electrochemical characteristics of nickel hydroxide are the key to the properties of the electrodes. Spherical nickel hydroxide powder, which suppresses the development of the inner pore volume and possesses a particle size distribution from several microns to tens of microns, makes it possible to increase the filling density and flowability of the active material. Thus, spherical nickel hydroxide can be more easily introduced into the three-dimensional porous nickel-foam substrates, and this is beneficial to the increase in the amount of the active material loaded in the electrode substrate and the improvement of energy density of the nickel electrodes. However, the electrochemical properties of spherical nickel hydroxide are not so good, e.g. the active material utilization, electronic conductivity and proton diffusion ability are quite low. So considerable interest has centred on the improvement of the electrochemical activity of nickel hydroxide. There are two approaches to enhance nickel hydroxide properties. (1) Modifying the nickel hydroxide with additives using different methods [6–11]. The modification methods can be the chemical coprecipitation doping of cobalt and zinc to $Ni(OH)_2$ crystalline lattice, the physical addition of nickel and cobalt metallic powders or cobalt compounds to $Ni(OH)_2$-based slurry, and the surface microencapsulation of $Ni(OH)_2$ powder with a thin layer of cobalt or nickel coatings by electroless deposition. (2) Controlling the microstructure of nickel hydroxide by changing the preparation techniques and synthesis parameters [12–17]. The electrochemical activity of nickel hydroxide materials is closely related to their microstructure and morphology. Studies [13, 16, 17] have shown that nickel hydroxide with a small crystallite size, a large number of structural defects, a high surface area and high degree of porosity has related indicators of superior electrochemical activity. The microstructure of nickel hydroxide is determined mainly by processing. Microstructure control by changing the synthesis methods has received particular attention for being effective on the improvement of the electrochemical properties. Several methods of nickel hydroxide synthesis have been developed, such as chemical precipitation [13], electrochemical deposition or electrosynthesis [18, 19], and the chimie douce technique [20]. Among these synthesis routes, the wet chemical precipitation is a convenient method to mass-produce powder materials, and it has been widely used to produce spherical nickel hydroxide powder which is the active material for pasted nickel electrodes.

In this paper, we have explored the second strategy described above and report on the synthesis and characterization of nanostructured nickel hydroxide material. Nanostructured powder has been synthesized by a chemical precipitation method with the aid of ultrasound, and the physical properties of the synthesized material were characterized and compared with those of the commercial spherical nickel hydroxide powder. The electrochemical properties of pasted nickel electrodes using a mixture of the nanostructured and spherical nickel hydroxide powders as the active material were investigated by charge/discharge tests and electrochemical impedance spectroscopy (EIS). The relationship between the structural characteristics and electrochemical activity of nickel hydroxide was also examined. The electrochemical properties of pasted nickel electrodes can be enhanced by adding an appropriate amount of nanostructured nickel hydroxide powder to spherical nickel hydroxide powder as the active material.

2. Experimental details

2.1. *Synthesis of nanostructured nickel hydroxide powder*

Nanostructured $Ni(OH)_2$ powder was synthesized via a wet chemical precipitation route. In the synthesis, predetermined amounts of $NiSO_4$ and NaOH solutions were fed by dripping into a reactor with vigorous stirring, and the temperature of the reactor was maintained at 50 °C. During the precipitation process, a surfactant (Polyoxyethylene sorbitan monooleate, Tween-80) and high-intensity ultrasound radiation (20 kHz, 100 W cm^{-2}) were used to prevent the newly produced $Ni(OH)_2$ microcrystals from growing and aggregating. After the precipitation process was complete, the precipitate was separated from the solution by centrifugation, washed repeatedly with distilled water, and then dried at 80 °C under vacuum.

2.2. *Physical characterization of nanostructured nickel hydroxide powder*

The crystallographic structure of $Ni(OH)_2$ powders was characterized by X-ray diffraction (XRD) with a Rigaku diffractometer using Cu$K\alpha$ radiation (λ=1.542 Å). Scanning electron microscopy (SEM) observation was performed using a LEO 1530 microscope. The specific surface area was evaluated by the Brunauer–Emmett–Teller (BET) nitrogen adsorption method using a CHEMBET-3000 surface area analyzer. Differential scanning calorimetry (DSC) analysis was carried out using a Shimadzu thermal analyzer with a heating rate of 10 °C min^{-1} in N_2. The filling density of the powders was obtained by tapping a measuring cylinder in which nickel hydroxide powders were packed. The flowability of the powders was evaluated through the measurement of angle of repose. The properties of the nanostructured $Ni(OH)_2$ powder were examined and compared with those of the commercial spherical $Ni(OH)_2$ powder.

2.3. *Electrochemical characterization of nanostructured nickel hydroxide powder*

Pasted nickel electrodes with an addition of nanostructured $Ni(OH)_2$ were prepared as follows: 5 wt.% nanostructured $Ni(OH)_2$ powder was mixed thoroughly with spherical $Ni(OH)_2$ powder as the active material, nickel and CoO powders were used as conductors, and a suitable amount of suspension containing 60 wt.% polytetrafluoroethylene (PTFE) and 1.5 wt.% carboxymethyl cellulose (CMC) was added to the mixed powders as a binder. The mixture was then blended to obtain a paste. The resulting paste was incorporated into a 2 cm × 2 cm nickel-foam substrate, to which a nickel ribbon was spot-welded as a current collector. Subsequently, the pasted electrodes were dried at 80 °C for 2–3 h and pressed at 175 MPa to assure good electrical contact between the substrate and the active material. For comparison, the nickel electrodes without the addition of nanostructured $Ni(OH)_2$ were also prepared using pure spherical $Ni(OH)_2$ powder as the active material.

Charge/discharge studies were conducted in a test cell, including the as-prepared nickel electrodes as the cathode and a hydrogen-storage alloy electrode as the anode. Polypropylene was used as the separator between the cathode and anode. The electrolyte solution consisted of 6 M KOH + 1 wt.% LiOH. The cell capacity was cathodically limited. The test cells were charged at a rate of 0.2 *C* for 7.5 h, and discharged to a cut-off voltage of 1.0 V at rates of 0.2, 0.5 and 1.0 *C*, respectively. Tests were performed on a Kikusui PF 40W-08 cycler.

For the electrochemical impedance spectroscopy (EIS) measurements, a three-compartment glass cell containing 6 M KOH + 1 wt.% LiOH electrolyte solution was used. The pasted nickel electrodes, which acted as the working electrode in the cell, were soaked in the electrolyte solution for 10 h before test. A hydrogen-storage alloy electrode with a capacity well in excess of the nickel electrodes was used as the counter electrode. For the reference electrode, a Hg/HgO (6 M KOH) electrode was employed, and the potential of the working electrode was monitored through a Luggin capillary with respect to the reference electrode. EIS studies were performed using an Autolab PGSTAT30 system. The impedance spectra were recorded at a 5 mV amplitude of perturbation, with a sweep frequency range of 20 kHz–1 mHz. All the electrochemical measurements were carried out at ambient temperature.

3. Results and discussion

3.1. *SEM and BET analyses*

Scanning electron micrographs at a high magnification for spherical and nanostructured $Ni(OH)_2$ powders are shown in Figure 1(a) and (b), respectively. It can be seen that $Ni(OH)_2$ particles consist of many tiny crystals. Spherical $Ni(OH)_2$ consists mainly of coarse crystals with sizes larger than 100 nm, while nanostructured $Ni(OH)_2$ contains many nanocrystals with sizes much smaller than 100 nm, and the size of pores included between these nanocrystals is also nanoscale. That is, nanostructured $Ni(OH)_2$ shows a nanocrystalline and nanoporous surface structure. From the BET measurement, the specific surface areas of spherical and nanostructured $Ni(OH)_2$ powders are 10 and 30 $m^2\ g^{-1}$, respectively. This indicates that nanostructured $Ni(OH)_2$ powder has a higher surface area, which can provide a high density of active sites and promote intimate interaction of the active material with the surrounding electrolyte. Therefore better utilization of the nanostructured $Ni(OH)_2$ material will be facilitated by a high specific surface area.

It is widely accepted that the nickel electrode works as an insertion electrode for protons. In the charge/discharge process, the redox reaction of Ni(II)/Ni(III) in alkaline media is believed to be a solid-state proton intercalation and de-intercalation [6, 12]. The electrochemical activity of nickel hydroxide materials can be improved by increasing the chemical proton diffusion coefficient in $Ni(OH)_2$. The nanoscale sizes of crystals and inner pores of nanostructured $Ni(OH)_2$ powder are beneficial to the acceleration of the solid-state proton diffusion in $Ni(OH)_2$, and this will diminish the concentration polarization of protons during charge/discharge, leading to better charge/discharge cycling behaviour. Thus, nanostructured $Ni(OH)_2$ is envisaged to display a superior electrochemical behaviour as compared to spherical $Ni(OH)_2$.

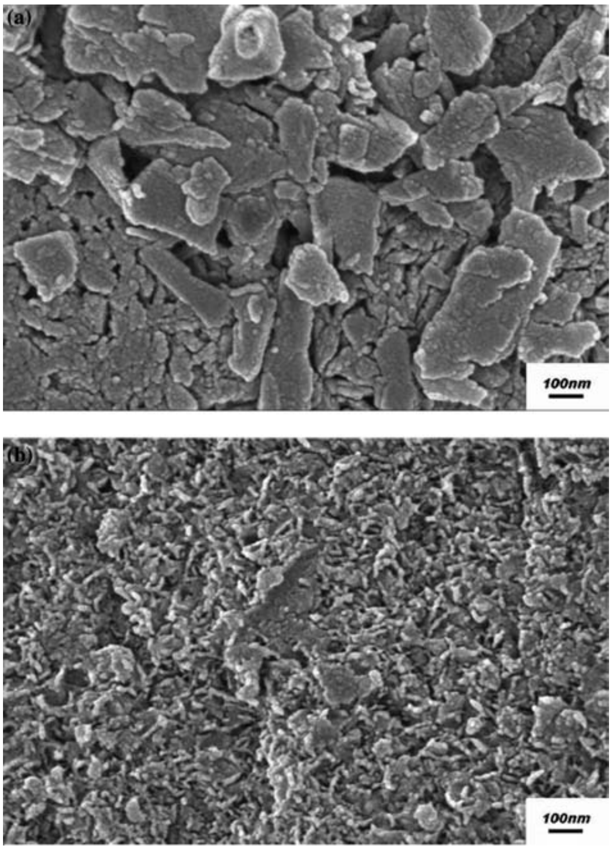

Fig. 1. SEM photographs for (a) spherical and (b) nanostructured $Ni(OH)_2$ powders.

3.2. *XRD patterns*

XRD patterns of spherical and nanostructured $Ni(OH)_2$ powders are presented in Figure 2(a) and (b) respectively. The crystal parameters obtained from XRD patterns are listed in Table 1. The characteristic diffraction peaks at (001), (100), (101), (102) and (110) show that both these $Ni(OH)_2$ samples have a β-type crystal structure. Compared with spherical $Ni(OH)_2$, nanostructured $Ni(OH)_2$ shows some different microstructural characteristics as revealed in the XRD patterns:

1. The peaks corresponding to the (001), (101) and (102) reflections in the XRD pattern of nanostructured $Ni(OH)_2$ are noticeably broadened as compared to those in the pattern of spherical $Ni(OH)_2$. The exceptional broadening of the (001), (101) and (102) reflection lines may be attributed to [16, 21, 22]: (i) crystallite size effects; (ii) increased degree of disordering on account of the existence of structural

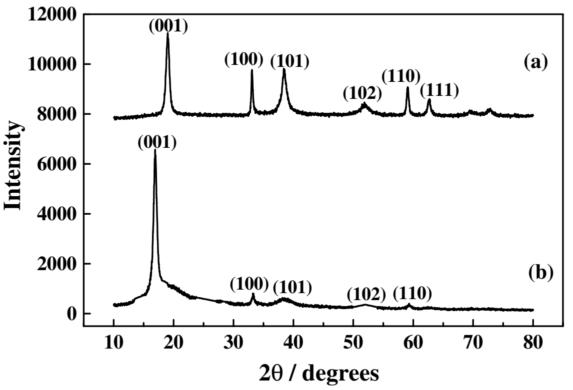

Fig. 2. XRD patterns for (a) spherical and (b) nanostructured $Ni(OH)_2$ powders.

defects, such as stacking faults/growth faults and proton vacancies, or the adsorption of inorganic species (water and anions); and/or (iii) the presence of other polymorphic modifications as inter-stratified phases. This suggests that nanostructured $Ni(OH)_2$ has a smaller crystallite size and more structural defects, which are advantageous to the improvement of electrochemical activity of the nickel hydroxide material. The crystallite sizes of nanostructured $Ni(OH)_2$ along the c- and a-axis are 2.5 and 2.3 nm respectively, as calculated from (001) and (100) XRD peaks using the Debye–Scherrer equation.

2. The (001) reflection line for nanostructured $Ni(OH)_2$ tends to shift to a lower angle, suggesting a larger lattice parameter of c_0 (5.23 Å). The shift in the position of the (001) peak probably results from the adsorption of the surfactant and water molecules in $Ni(OH)_2$. The c_0 value corresponds to the inter-sheet distance of a layered structure of $Ni(OH)_2$. Thus, an expanded inter-sheet distance is obtained with nanostructured $Ni(OH)_2$ as related to spherical $Ni(OH)_2$. Studies have indicated that the large c_0 promoted the adsorption and/or incorporation of anions and water molecules in $Ni(OH)_2$, which could facilitate the intercalation and de-intercalation reaction of protons in the $Ni(OH)_2$ lattice [12, 20, 23–26]. So nanostructured $Ni(OH)_2$ with a larger c_0 is expected to exhibit a faster proton diffusion process and better high-rate charge/discharge behaviour.

Table 1. Experimental results of XRD analysis for nickel hydroxide powders

Parameters	Nanostructured $Ni(OH)_2$	Spherical $Ni(OH)_2$
Crystal type	β-$Ni(OH)_2$	β-$Ni(OH)_2$
Crystallite size calculated from (001) peak/nm	2.5	13.0
Crystallite size calculated from (100) peak/nm	2.3	12.0
Lattice parameter a_0/Å	3.11	3.13
Lattice parameter c_0/Å	5.23	4.61

3.3. *DSC curves*

Previous studies on heating nickel hydroxide materials have postulated two categories of chemical reaction [5, 27]. One process is dehydration (Equation 1) which corresponds to the loss of the adsorbed and/or structurally bonded water below 250 °C, and the other is decomposition of nickel hydroxide to nickel oxide (Equation 2) when $Ni(OH)_2$ is heated above 250 °C.

Dehydration reaction:

$$Ni(OH)_2 \cdot X_w H_2O \rightarrow Ni(OH)_2 + X_w H_2O, \qquad (1)$$

where X_w is the moles of water.

Decomposition reaction:

$$Ni(OH)_2 \rightarrow NiO + H_2O \qquad (2)$$

DSC curves for spherical and nanostructured $Ni(OH)_2$ are shown in Figure 3(a) and (b) respectively. The temperatures corresponding to the endothermic peaks of the decomposition reaction are 322.1 and 315.1 °C for spherical and nanostructured $Ni(OH)_2$, respectively. As indicated by SEM and XRD analyses, nanostructured $Ni(OH)_2$ has a smaller crystallite size than that of spherical $Ni(OH)_2$. Thus, it is found that nanostructured $Ni(OH)_2$ with a smaller crystallite size possesses a lower

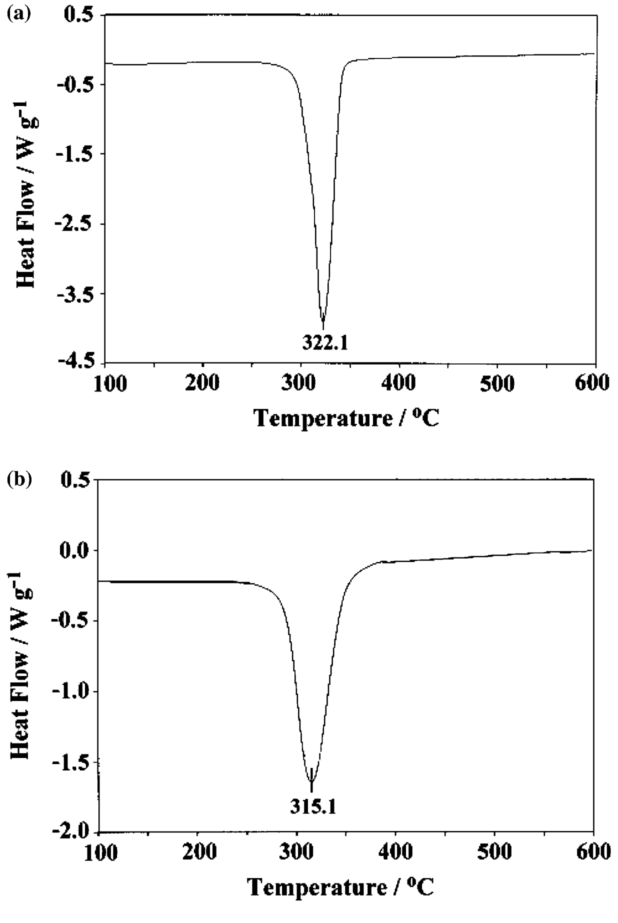

Fig. 3. DSC curves for (a) spherical and (b) nanostructured $Ni(OH)_2$ powders.

thermal decomposition temperature. Such a relationship between the decomposition temperature and the crystallite size of nickel hydroxide materials was also observed by Watanabe et al. [6]. So the lowering of the thermal decomposition temperature is also beneficial to the electrochemical activity of nanostructured $Ni(OH)_2$.

3.4. *Filling density and flowability of nickel hydroxide powders*

To investigate the filling density and flowability of nickel hydroxide powder materials, the tapping density and angle of repose were measured, and the results are shown in Table 2. Nanostructured $Ni(OH)_2$ shows a larger angle of repose and a lower tapping density as compared with spherical $Ni(OH)_2$. This suggests that the filling property and flowability of the nanostructured powder are inferior to those of the spherical powder.

The pasted foam-nickel electrodes with spherical $Ni(OH)_2$ powder as the active material have been widely used in commercially available Ni/MH and Ni/Zn batteries. It is necessary for the preparation of high energy density electrodes to increase the amount of active material powder loaded in the three-dimensional porous nickel-foam substrate. Thus, a high filling density and good flowability are required.

As indicated by SEM, XRD and DSC studies, nanostructured $Ni(OH)_2$ is envisaged to exhibit a superior electrochemical behaviour as related to spherical $Ni(OH)_2$. Thus an effective way of improving the performance of pasted nickel electrodes is to use a mixture of the nanostructured and spherical $Ni(OH)_2$ powders as the active material, which can fully utilize the individual property advantages of these two powder materials. This conclusion is corroborated by the charge/discharge and EIS studies.

3.5. *Charge/discharge tests for pasted nickel electrodes*

Figure 4 shows typical discharge curves at the 1.0 *C* rate for the pasted nickel electrode with pure spherical $Ni(OH)_2$ as active material (code A) and the electrode with an addition of 5 wt.% nanostructured $Ni(OH)_2$ to spherical $Ni(OH)_2$ (code B). It can be seen that the depth-of-discharge (DOD) and discharge capacity of the electrode B are larger than those of the electrode A. Moreover, the discharge voltage of electrode B is also higher than that of electrode A. Table 3 gives the specific discharge capacities of $Ni(OH)_2$ at various discharge rates for electrodes A and B. The results show that the addition of nanostructured $Ni(OH)_2$ powder considerably increases the specific discharge capacity and active material utilization of spherical $Ni(OH)_2$ powder, and the effects become more notable with the increase in discharge rate. This indicates that the addition of nanostructured $Ni(OH)_2$ to spherical $Ni(OH)_2$ not only increases the electrochemical activity and utilization of the nickel hydroxide active material, but also improves the high-rate capability.

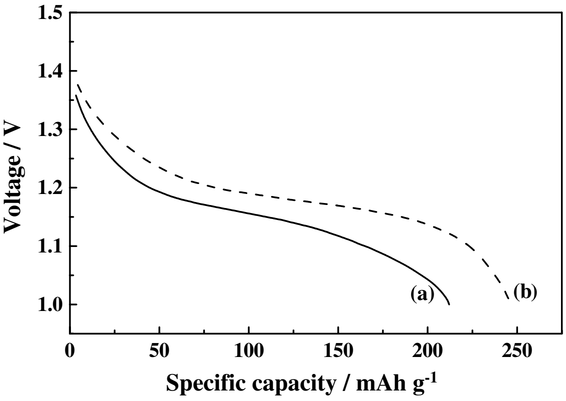

Fig. 4. Typical discharge curves at the 1.0 *C* rate for pasted nickel electrodes: (a) without and (b) with an addition of 5 wt.% nanostructured $Ni(OH)_2$ powder.

3.6. *EIS measurements of pasted nickel electrodes*

Figure 5 shows the electrochemical impedance spectra for the pasted nickel electrodes A and B. The impedance spectra display a depressed semicircle resulting from the charge transfer resistance in the high-frequency region, and a slope related to the Warburg impedance appearing in the low-frequency region. It can be seen that the impedance of electrode B with the addition of nanostructured $Ni(OH)_2$ is smaller than that of electrode A without nanostructured $Ni(OH)_2$. This implies that the electrochemical reaction on electrode B proceeds more easily than that on electrode A.

In comparison with spherical $Ni(OH)_2$, nanostructured $Ni(OH)_2$ possesses a higher surface area, a smaller crystallite size and more structural defects. Therefore, the addition of nanostructured $Ni(OH)_2$ to spherical $Ni(OH)_2$ can provide an optimal degree of contact between the electrode and the electrolyte, and facilitate the intercalation/de-intercalation of protons or the rapid

Table 2. Angle of repose and tapping density of nickel hydroxide powders

Property parameters	Nanostructured $Ni(OH)_2$	Spherical $Ni(OH)_2$
Angle of repose/degrees	117	49.2
Tapping density/g ml^{-1}	1.53	2.16

Table 3. Specific discharge capacities of $Ni(OH)_2$ at various discharge rates for pasted nickel electrodes

Nickel electrodes	Specific discharge capacity/mAh (g^{-1} $Ni(OH)_2$)		
	0.2 *C*	0.5 *C*	1.0 *C*
Electrode A	272	245	212
Electrode B	286	270	247

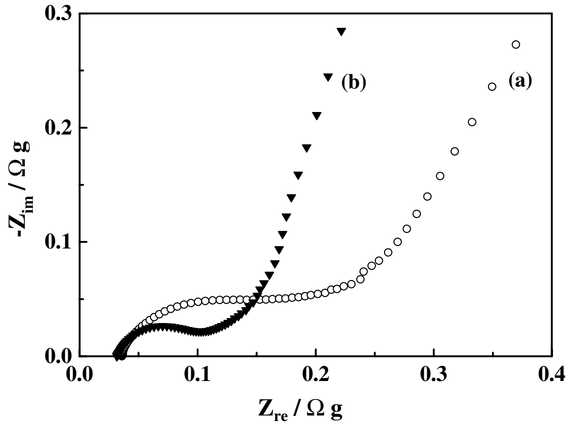

Fig. 5. Electrochemical impedance spectra of pasted nickel electrodes: (a) without and (b) with an addition of 5 wt.% nanostructured $Ni(OH)_2$ powder.

movement of both electrons and protons in the electrode. Accordingly, a higher discharge capacity and better high-rate capability can be obtained for the electrode with added nanostructured $Ni(OH)_2$.

4. Conclusions

Nanostructured nickel hydroxide powder can be synthesized by a wet chemical precipitation method with the aid of ultrasound. It is confirmed that the nanostructured nickel hydroxide is crystalline β-$Ni(OH)_2$ with a nanocrystalline and nanoporous surface structure. Compared with commercial spherical β-$Ni(OH)_2$, nanostructured β-$Ni(OH)_2$ possesses a smaller crystallite size, more structural defects, a larger lattice parameter of c_0, a higher specific surface area and lower thermal decomposition temperature. The crystallite sizes of nanostructured $Ni(OH)_2$ along the *c*- and *a*-axis are 2.5 and 2.3 nm, respectively. These physical characteristics are advantageous to the improvement of electrochemical activity of the nanostructured $Ni(OH)_2$ powder.

The filling density and flowability of nanostructure $Ni(OH)_2$ are inferior to those of spherical $Ni(OH)_2$. Electrochemical measurements reveal that the pasted nickel electrode using a mixture of the nanostructured and spherical $Ni(OH)_2$ powders as the active material exhibits superior electrochemical performance in comparison with that of the electrode prepared with pure spherical $Ni(OH)_2$. That is, a higher discharge capacity and discharge voltage, better high-rate capability and a lower electrochemical reaction impedance can be obtained with the nickel electrode with added nanostructured $Ni(OH)_2$. Thus the performance of pasted nickel electrodes can be improved by adding an appropriate amount of nanostructured $Ni(OH)_2$ powder to spherical $Ni(OH)_2$ powder as the active material.

References

1. S.R. Ovshinsky, M.A. Fetcenko and J. Ross, *Science* **260** (1993) 176.
2. K. Ota, S. Mitsushima, S. Kato, S. Asano, H. Yoshitake and N. Kamiya, *J. Electrochem. Soc.* **139** (1992) 667.
3. V. Srinivasan and J.W. Weidner, *J. Electrochem. Soc.* **147** (2000) 880.
4. A.M. Couper, D. Pletcher and F.C. Walsh, *Chem. Rev.* **90** (1990) 837.
5. C. Natarajan, H. Matsumoto and G. Nogami, *J. Electrochem. Soc.* **144** (1997) 121.
6. K. Watanabe, T. Kikuoka and N. Kumagai, *J. Appl. Electrochem.* **25** (1995) 219.
7. I. Munehisa and A. Norikatsu, Eur. Patent No. EP 0523284 (1993).
8. K. Watanabe, M. Koseki and N. Kumagai, *J. Power Sources* **58** (1996) 23.
9. M. Oshitani, H. Yufu, K. Takashima, S. Tsuji and Y. Matsuma, *J. Electrochem. Soc.* **136** (1989) 1590.
10. A.B. Yuan and N.X. Xu, *J. Appl. Electrochem.* **31** (2001) 245.
11. M.S. Wu, C.M. Huang, Y.Y. Wang and C.C. Wan, *Electrochim. Acta* **44** (1999) 4007.
12. P. Oliva, J. Leonardi, J.F. Laurent, C. Delmas, J.J. Braconnier, M. Figlarz, F. Fievet and A. Guibert, *J. Power Sources* **8** (1982) 229.
13. P.V. Kamath and G.N. Subbanna, *J. Appl. Electrochem.* **22** (1992) 478.
14. P.V. Kamath, M. Dixit, L. Indira, A.K. Shukla, V.G. Kumar and N. Munichandraiah, *J. Electrochem. Soc.* **141** (1994) 2956.
15. M. Dixit, P.V. Kamath and J. Gopalakrishnan, *J. Electrochem. Soc.* **146** (1999) 79.
16. C. Tessier, P.H. Haumesser, P. Bernard and C. Delmas, *J. Electrochem. Soc.* **146** (1999) 2059.
17. R.S. Jayashree, P.V. Kamath and G.N. Subbanna, *J. Electrochem. Soc.* **147** (2000) 2029.
18. R.S. Jayashree and P.V. Kamath, *J. Appl. Electrochem.* **29** (1999) 449.
19. R.S. Jayashree and P.V. Kamath, *J. Power Sources* **93** (2001) 273.
20. L. Demourgues-Guerlou and C. Delmas, *J. Power Sources* **45** (1993) 281.
21. Q.S. Song, Z.Y. Tang, H.T. Guo and S.L.I. Chan, *J. Power Sources* **112** (2002) 428.
22. S. Deabate, F. Fourgeot and F. Henn, *J. Power Sources* **87** (2000) 125.
23. C. Faure, C. Delmas and M. Fouassier, *J. Power Sources* **35** (1991) 279.
24. R.S. Jayashree and P.V. Kamath, *J. Appl. Electrochem.* **31** (2001) 1315.
25. P.V. Kamath and N.Y. Vasanthacharya, *J. Appl. Electrochem.* **22** (1992) 483.
26. M.C. Bernard, R. Cortes, M. Keddam, H. Takenouti, P. Bernard and S. Senyarich, *J. Power Sources* **63** (1996) 247.
27. B. Mani and J.P. Neufville, *J. Electrochem. Soc.* **135** (1988) 800.